International Journal of Nanomedicine

Dovepress
open access to scientific and medical research

Open Access Full Text Article

ORIGINAL RESEARCH

Multidynamic Osteogenic Differentiation by Effective Polydopamine Micro-Arc Oxide Manipulations

Yuqi Zhou[1,*], Guifang Wang[2,*], Tianqi Wang[1], Jiajia Wang[3], Xutao Wen[3], Haishui Sun[1], Lei Yu[1], Xiaoying Liu[4], Juanjuan Zhang[1], Qin Zhou[3], Yan Sun[1]

[1]School of Stomatology, Weifang Medical University, Weifang, People's Republic of China; [2]Department of Prosthodontics, Ninth People's Hospital, Shanghai Jiaotong University School of Medicine, College of Stomatology, Shanghai Jiao Tong University, National Center for Stomatology, National Clinical Research Center for Oral Diseases, Shanghai Key Laboratory of Stomatology, Shanghai, People's Republic of China; [3]Department of Oral Surgery, Ninth People's Hospital, Shanghai Jiaotong University School of Medicine, College of Stomatology, Shanghai Jiao Tong University, National Center for Stomatology, National Clinical Research Center for Oral Diseases, Shanghai Key Laboratory of Stomatology, Shanghai, People's Republic of China; [4]School of Bioscience and Technology, Weifang Medical University, Weifang, People's Republic of China

*These authors contributed equally to this work

Correspondence: Qin Zhou, Department of Oral Surgery, Ninth People's Hospital, Shanghai Jiaotong University School of Medicine, College of Stomatology, Shanghai Jiao Tong University, National Center for Stomatology, National Clinical Research Center for Oral Diseases, Shanghai Key Laboratory of Stomatology, Shanghai, 200011,People's Republic of China, Tel +86 15900827810, Email qin_zq@163.com; Yan Sun, School of Stomatology, Weifang Medical University, Weifang, Shandong Province, 261053, People's Republic of China, Tel +86 13356797219, Email sunyan@wfmc.edu.cn

Introduction: The nanostructural modification of the oral implant surface can effectively mimic the morphology of natural bone tissue, allowing osteoblasts to achieve both proliferation and differentiation capabilities at the bone interface of the dental implant. To improve the osteoinductive activity on the surface of titanium implants for rapid osseointegration, we prepared a novel composite coating (MAO-PDA-NC) by micro-arc oxidation technique and immersion method and evaluated the proliferation, adhesion, and osteogenic differentiation of osteoblasts on this coating.

Methods: The coatings were prepared by micro-arc oxidation (MAO) technique and immersion method, and characterized by scanning electron microscopy (SEM) and atomic force microscopy (AFM) for different coatings; the loading of PDA was examined using Fourier transform infrared spectroscopy (FTIR); the ion release capacity of the coatings was determined by inductively coupled plasma emission spectrometry (ICP-OES); the interfacial bonding of the coatings was examined using nanoscratch experiment strength. The cytotoxicity of the coating was examined by live/dead staining kit; cell proliferation viability was examined by CCK-8 kit; adhesion and osteogenic effect of the coating were examined by immunofluorescence staining and RT-PCR; osteogenic differentiation was examined by alkaline phosphatase staining.

Results: The surface morphology of titanium implants was modified by micro-arc oxidation technology, and a new MAO-PDA-NC composite coating was successfully prepared. The results showed that the MAO-PDA-NC coating not only optimized the physical and chemical properties of the titanium implant surface but also significantly stimulated the biological properties of osteoblast adhesion, proliferation, and osteogenic differentiation on the coating surface.

Conclusion: These results show that MAO-PDA-NC composite coating can significantly improve the surface properties of titanium implants and achieve a stable bond between implant and bone tissue, thus accelerating early osseointegration.

Keywords: proliferation, differentiation, micro-arc oxidation, osseointegration

Introduction

With the development of biomaterials and the advancement of multifunctional technologies, new materials for oral implants have become commonplace and are gradually coming to the attention of oral implantologists. Currently, titanium and its alloys are widely used for dental implants as a biocompatible material with good mechanical properties

Received: 22 June 2022
Accepted: 6 September 2022
Published: 11 October 2022

as well as corrosion resistance.[1] However, the surface of titanium-based materials is biologically inert and has limited ability to induce new bone formation for ideal osseointegration.[2] Therefore, how to achieve rapid as well as better osseointegration is a major challenge for contemporary dental implantologists and researchers.

The development of a new generation of titanium implant surfaces that are biologically active and promote osseointegration has been a hot topic of research, the key point of which is that the modified titanium implant surface is closer to the natural bone tissue morphology and chemical properties, which can provide the growth environment required for bone regeneration.[3] Several methods based on optimizing the surface properties of titanium implants, including changing the surface morphological structure and optimizing the surface chemistry, can effectively modulate the osseointegration at the interface of titanium implant materials.[4–6] Among the means of titanium surface coating modification, the micro-arc oxidation (MAO) method is to form a porous, rough titanium oxide coating on the titanium surface and to dope the Ca and P elements in the electrolyte into the coating, thus giving the implant a larger contact area with the surrounding bone tissue and imparting osteogenic activity to the coating.[7]

The incorporation of bioactive materials into the MAO-coated surface is a promising approach. The incorporation of biomaterials can further optimize the biological activity of implant implants, improve osteoinduction and shorten the period of osseointegration. In recent years, nanoclay has proven to be an attractive bioactive material for bone tissue engineering and is widely used in various biomedical research.[8,9] On the one hand, nanoclays are composed of simple or complex layered silicates with good biocompatibility as well as osteogenic induction capabilities. For example, synthetic silicate nanoplates can induce osteogenic differentiation of human bone marrow mesenchymal stem cells (hBMSCs) in the absence of osteogenic inducing factors or bioactive molecules.[10] Compared with collagen-based hydrogels, collagen hydrogels containing two-dimensional nanosilicates can enhance the formation of the mineralized matrix required for bone tissue growth, thereby promoting the bone regenerative capacity and showing great promise for application in bone tissue engineering.[11] On the other hand, nanoclay has an inhomogeneous charge distribution as well as a high surface-to-volume ratio that can facilitate chemical bonding or physical adsorption with biopolymers.[8] Therefore, nanoclay is often used to cross-link various polymers, such as polydopamine (PDA), and interact with them to form hydrogels with a double network structure, improving physical and mechanical properties.[12] PDA is a black-brown coating produced by the aerobic weak base environment of dopamine with extremely strong adhesion properties and various active functional groups.[13,14] Among them, the highly transitive catechol and amine functional groups on the PDA chains not only enhance the interfacial interactions between the clay nanosheets and the polymer network through physical cross-linking but also achieve functional coating loading by non-covalent and covalent chemical reactions with the substrate.[15,16] For example, the optimal combination of high adhesion and toughness was achieved by a two-step preparation of polydopamine clay polyacrylamide (PDA-clay-PAM) hydrogels, and the excellent adhesion properties of this hydrogel were attributed to nanoclay-induced PDA oxidation, which maintained a large number of free catechol groups in the hydrogel. Also, the toughness of this hydrogel may be attributed to the presence of covalent and non-covalent cross-linked PDA polymer networks and nanoclay reinforcements. In addition, cellular experiments demonstrated that the PDA-clay-PAM hydrogel facilitated cell adhesion and proliferation with good cell affinity.[16] Therefore, strategies that mimic PDA adhesion to overcome the limitations of cell and tissue repulsive hydrogels, titanium implants, and scaffold materials introduce important advances in the design of biomaterials with adequate adhesion and excellent mechanical properties.

In this study, we chose the MAO technique as a method to fabricate dental implants to form microporous structures on titanium surfaces for a variety of material surfaces. Based on the mussel-inspired PDA adhesion mechanism, we embedded dopamine powder into the nanoclay layer on the MAO coating surface to confine dopamine oxidation to the clay layer space, thus forming a PDA clay layer rich in catecholamine moieties on the MAO coating surface (MAO-PDA-NC coating). We further investigated the activity, adhesion and osteogenic differentiation of osteoblasts on this coating to provide an experimental basis for early and rapid osseointegration of titanium implants in a clinical setting.

Materials and Methods

Preparation of Materials

The titanium sheets (10 mm × 10 mm × 1 mm) used in this study were obtained from commercially pure titanium sheets. The surface of the titanium sheet was sandpapered and polished, and then gradually cleaned with acetone, anhydrous

ethanol, and deionized water in an ultrasonic cleaning machine in turn. Firstly, to prepare the micro-arc oxidation coatings, the samples were prepared as porous surface layers by micro-arc oxidation in an electrolyte solution consisting of 35.2 g/L of calcium acetate monohydrate ($C_4H_6CAO_4H_2O$, Macklin, Shanghai, China) and 12.24 g/L of sodium pentahydrate β-glycerophosphate ($C_3H_7NA_2O_6P{\cdot}5(H_2O)$, Aladdin, Shanghai, China). Secondly, MAO-PDA coatings were prepared. Dopamine hydrochloride powder (Aladdin, Shanghai, China) was added to 10 mM Tris-HCl buffer solution (pH = 8.5, Aladdin, Shanghai, China) at a concentration of 2 mg/mL and stirred continuously for 24 h to obtain a black PDA solution.[13] Then, the MAO samples were soaked in the PDA solution overnight away from light, thus obtaining the MAO-PDA coating. Finally, preparation of MAO-PDA-NC coating, Halloysite nanoclay (Aladdin, Shanghai, China) at 35 mg/ml was added to 10 mM of Tris-HCl buffer and the solution was put into a constant temperature stirrer for 2 h. Subsequently, dopamine hydrochloride powder was added and stirring was continued. The MAO samples were put into overnight immersion protected from light to obtain MAO-PDA-NC coating.

Material Surface Characteristics

To analyze the physical characteristics of the material surface, the surface morphology and pore size of the samples were analyzed by scanning electron microscopy (SEM, Hitachi, 3400N, Japan), and the chemical composition of the coatings was analyzed using an energy-dispersive X-ray spectroscopy(EDS, Bruker, Germany), and the surface roughness of the coatings was evaluated using an atomic force microscope (AFM, Bruker, Germany). And the Fourier transform infrared spectroscopy (FTIR, Thermo Scientific Nicolet iS20, USA) spectra of the dried samples were obtained using a PerkinElmer Spectrum One spectrometer, the wetting properties of the coating surfaces were assessed using a contact angle meter (SL200B, Solon, China), and inductively coupled plasma/optical emission spectroscopy (ICP-OES, PerkinElmer Avio 200, USA) was used to analyze the ion release from the different coatings. Nanoscratcher (Hysitron TI 950, USA) detects the integrated load-bearing capacity between MAO+PDA+NC coating and the base system to obtain the interfacial bond strength magnitude.

Cell Culture of Rat BMSCs

The Sprague Dawley (SD) rats used in the experiments were obtained from the Animal Centre of the Ninth People's Hospital of Shanghai Jiao Tong University, and animal ethical approval was obtained for all animal experiments performed. Primary bone marrow mesenchymal stem cells were isolated from selected 3-week-old Sprague Dawley male rats. Rats were executed by spinal dislocation and the tibia and femur were removed under aseptic conditions, and rat bone marrow mesenchymal stem cells (rBMSCs) were collected and repeatedly washed with a culture medium, centrifuged, and suspended. The culture medium was changed every other day until the cells reached 80–90% for passage, and the 2nd-4th generation cells were selected for subsequent experiments. The cells used in this study were cultured and expanded in Dulbecco's modified Eagle's medium (DMEM, HyClone, Logan, UT) with 10% fetal bovine serum (FBS), 1% penicillin/streptomycin (Gibco, Carlsbad, CA) and cultured at 37 °C in a 5% CO_2 humidified environment.

Live/Dead Fluorescence Staining and Cell Counting Kit-8 (CCK-8) Assay

To assess the cell viability on different samples, the live-dead cell staining solution (Beyotime, Cat: C2015M, Shanghai, China) was applied to detect cell activity and cytotoxicity. Briefly, 2.0×10^4 cells/well were inoculated on the samples. After 24 h of incubation, the culture medium was discarded, the cells were washed with PBS, and the appropriate volume of assay working solution was added and incubated at 37 °C for 30 min. Cells were observed by fluorescence microscopy (Olympus, Tokyo, Japan) immediately after the incubation.

Cells were inoculated on different samples as described previously and after 1, 3, and 5 days of incubation, the medium was mixed with CCK-8 reagent (DOJINDO, Kumamoto, Japan) in a 10:1 ratio and added to 24-well plates and incubated for 1.5 h. Subsequently, 100 μL/well supernatant was pipetted to a 96-well plate, and the absorbance was measured at 450 nm using an enzyme analyzer. The experiments were performed three times.

To observe the morphological characteristics of BMSCs on the material surface, the cytoskeleton was determined by staining with tetramethylrhodamine (TRITC)-globulin. BMSCs were inoculated at a density of 5×10^4/well and cultured on different samples. After 24 h of incubation, 4% paraformaldehyde was fixed and 0.5% Triton X-100 was

permeabilized. Subsequently, they were sealed with bovine serum albumin (BSA). Finally, TRITC (Yeasen, Shanghai, China) was used to label the cytoskeleton and DAPI (Solarbio, Beijing, China) to label the nucleus. Images were taken under a fluorescence microscope (TE2000-U, Nikon, Tokyo, Japan).

Cell Adhesion Examination of Different Coatings

Cells were cultured on different samples for 3 days and immunofluorescence staining was performed to observe the expression of the Vinculin gene. Cells were fixed with 4% paraformaldehyde and washed with PBS; subsequently, 0.5% Triton X-100 was permeabilized and incubated with 5% bovine serum protein for 1 h. Primary antibodies specific for Vinculin (Beyotime, Shanghai, China) were first incubated on the cells overnight and then on Alexa Fluor 488 AffiniPure Donkey anti-Rabbit IgG (H+L) antibody (Yeasen, Shanghai, China) for 1 h. The cytoskeletal structures were stained with TRITC phalloidin and nuclear staining was performed with DAPI. A fluorescence microscope (TE2000-U, Nikon, Tokyo, Japan) was used for measurements.

To further examine cell adhesion on different samples, the expression of Integrin adhesion-associated genes was detected by reverse transcriptase-polymerase chain reaction (RT-PCR). Cells were inoculated with 5×10^4 /well on 24-well plates and cultured in DMEM medium for 7 days before total cellular RNA was extracted using Trizol reagent (Invitrogen, Grand Island, NJ). Integrin adhesion-associated genes Integrin β3, Integrin α2, Integrin α3, and Integrin α4 expression was assessed by real-time PCR using SYBR Premix Ex Taq II (Takara). The relative expression levels of each related gene were normalized to the relative expression levels of the housekeeping gene GAPDH as described above. The primer sequences of the genes mentioned in the experiments are shown in Table 1.

Osteogenic Performance Analysis of Different Coatings

The expression of osteogenic genes was detected by reverse transcriptase-polymerase chain reaction (RT-PCR). Cells were inoculated with 5×10^4 /well on 24-well plates and cultured in DMEM medium for 7 days before total cellular RNA was extracted using Trizol reagent (Invitrogen, Grand Island, NJ). Expression of the osteogenesis-related genes ALP, OPN, Runx2, and OSX was assessed by real-time PCR using SYBR Premix Ex Taq II (Takara). The primer sequences of the genes mentioned in the experiments are shown in Table 2.

Immunofluorescence was used to detect the expression of Runx2, OCN and OPN. Cells were inoculated with 5×10^4 /well on 24-well plates and cultured in DMEM medium for 5 days. Cells were fixed with 4% paraformaldehyde and washed with PBS; subsequently, 0.5% Triton X-100 was permeabilized and incubated with 5% bovine serum protein for 1 h. Primary antibodies specific for Runx2 (Cell Signaling Technology, Shanghai, China), OCN (Beyotime, Shanghai, China) and OPN (Beyotime, Shanghai, China) were first incubated on the cells overnight and then on Alexa Fluor 488 AffiniPure Donkey anti-Rabbit IgG (H+L) antibody (Yeasen, Shanghai, China) for 1 h. The cytoskeletal structures were stained with TRITC phalloidin and nuclear staining was performed with DAPI. A fluorescence microscope (TE2000-U, Nikon, Tokyo, Japan) was used for measurements.

Alkaline phosphatase (ALP) staining and ALP activity analysis were used to verify the osteogenic effect. 5×10^4 cells/well were inoculated in 24-well plates containing osteogenic medium and cultured for 14 days before fixation and staining of the cells using an alkaline phosphatase kit (Beyotime Biotechnology, Shanghai, China), and the samples were observed under a microscope for staining. Semi-quantitative analysis of alkaline phosphatase was performed to determine alkaline phosphatase activity by measuring the OD value of absorbance at 405 nm. Total protein values were measured at 562 nm

Table 1 Primers for the Expression of Adhesion-Related Genes in BMSCs

Gene	Forward Primer Sequence	Reverse Primer Sequence
Integrin β3	CCGTGACGAGATTGAGTCA	AGGATGGACTTTCCACTAGAA
Integrin α2	GGAACGGGACTTTCGCAT	GGTACTTCGGCTTTCTCATCA
Integrin α3	AAGGGACCTTCAGGTGCA	TGTAGCCGGTGATTTACCAT
Integrin α4	GCTTCTCAGATCTGCTCGTG	GTCACTTCCAACGAGGTTTG
GAPDH	GACATCAAGAAGGTGGTGAAGC	TGTCATTGAGAGCAATGCCAGC

Table 2 Primers for the Expression of Osteogenesis-Related Genes in BMSCs

Gene	Forward Primer Sequence	Reverse Primer Sequence
ALP	GGGACTGGTACTCGGACAAT	GGCCTTCTCATCCAGTTCAT
OPN	GACGATGATGACGACGACGATGAC	GTGTGCTGGCAGTGAAGGACTC
OCN	GGTGCAGACCTAGCAGACACCA	AGGTAGCGCCGGAGTCTATTCA
OSX	CGGCAAGGTGTACGGCAAGG	GAGCAGAGCAGACAGGTGAACTTC
Runx2	ACAACCACAGAACCACAAG	TCTCGGTGGCTGGTAGTGA
GAPDH	GACATCAAGAAGGTGGTGAAGC	TGTCATTGAGAGCAATGCCAGC

using the Bio-Rad protein analysis kit. The results of the alkaline phosphatase analysis were normalized and expressed as total protein OD per mg of cells.

Analysis of the Osteogenic Properties of Sample Extracts

Four different groups of samples were placed in the serum-free and double antibodies-free medium for 7 days, and the extracts were subsequently collected for subsequent experiments. A control group (cultured in a normal medium) as well as TI, MAO, MAO+PDA, and MAO+PDA+NC extract groups were established by adding 10% serum as well as 1% double antibodies to the extracts. RT-PCR, ALP activity assays, as well as OPN (Beyotime, Shanghai, China) immunofluorescence staining were performed to assess the osteogenic potential of ions released from the extracts of different samples.

Statistical Analysis

All of the above experiments were repeated at least three times, and the results were expressed as mean ± standard deviation (SD). They analyzed the results using Origin (Origin Lab Corporation, North Hampton) software. One-way analysis of variance and multiple comparison tests were used to determine statistical significance. Statistically significant differences between groups and controls are indicated by "*". "NS" indicates no significant difference.

Results

Characterization and Properties of Different Coatings

MAO technique was used to treat titanium flakes and different MAO-active coatings were prepared by adding PDA and Nanoclay components. Surface morphological characteristics between the different samples using SEM, and it was found that MAO, MAO+PDA, and MAO+PDA+NC coatings had relatively simple textures as well as micron/nanometer pits that provided transport channels for cell, energy, and nutrient uptake (Figure 1A). Observation of porosity and pore size of the different samples (Figure 1B and C), and the results showed that there was no significant difference in the shape and size of the micro/nanoscale particles between the groups. The 3D morphology and roughness of the different samples were observed using AFM. Among them, the surface roughness of TI was 228 nm, while the surface roughness of the MAO, MAO+PDA, and MAO+PDA+NC group were 377.9, 401.7, and 553.8 nm, respectively. The MAO+PDA+NC coating formed a rougher surface compared to the other groups, while there was no significant difference between MAO and MAO+PDA groups (Figure 1D and E). It was shown that the surface morphology of titanium treated by microarc oxidation underwent significant changes, forming micro/nanostructures, while the surface roughness was altered by the addition of nanomaterials, thus promoting the normal biological function of osteoblasts.

EDS evaluated the surface elemental composition of the different samples. During the micro arc oxidation process, the Ca and P elements from the electrolyte were successfully incorporated into the generated oxide layer to form different MAO active coatings. Among them, the chemical compositions of the MAO and MAO+PDA groups were consistent (Figure 2A), probably because PDA is mostly attached to the surface of titanium sheets by coordination and/or chelation of catechol groups, and its chemical composition is similar to that of true melanin in nature. Halloysite nanoclay, a member of the montmorillonite mineral family, consists of silicate crystals rich in a variety of chemical elements. Not only Ca and P elements in the electrolyte could be observed in the MAO+PDA+NC coating, but also Al and Si elements were found, indicating that nanoclay was successfully loaded on the coating surface (Figure 2A and B).

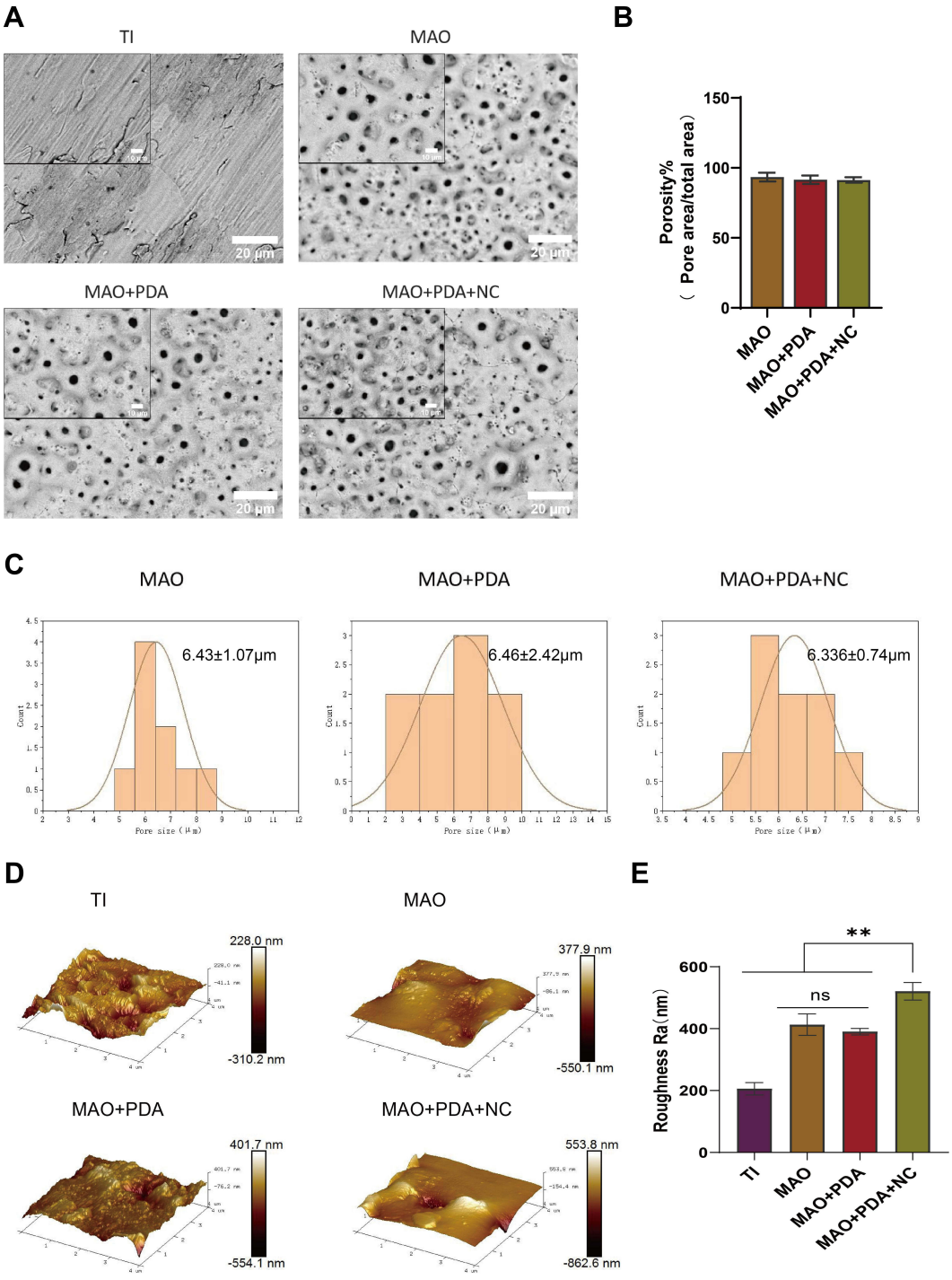

Figure 1 Characterization of the templates.

Notes: (**A**) Surface morphology of TI, MAO, MAO+PDA, and MAO+PDA+NC was observed by the SEM. (**B**) Surface porosity distribution of MAO, MAO+PDA, and MAO +PDA+NC coating. (**C**) Frequency distribution of surface aperture in MAO, MAO+PDA, and MAO+PDA+NC. (**D**) AFM images showing three-dimensional structures of TI, MAO, MAO+PDA, and MAO+PDA+NC. (**E**) Quantitative evaluation of coating surface roughness (Ra). Scale bar: 10 and 20μm.

The water contact angle is used to determine the hydrophilic state of the surface interface of the coating. The surface contact angles of the TI, MAO, MAO+PDA and MAO+PDA+NC groups were 49.24°, 42.14°, 7.74°, and 10.12°, respectively (Figure 3A and B). The results showed that the contact angle decreased and the hydrophilicity increased in the different MAO active coating groups compared to the pure TI group. With the addition of PDA coating, the material surfaces of MAO+PDA and MAO+PDA+NC groups have smaller contact angles, which indicates that the contact angle

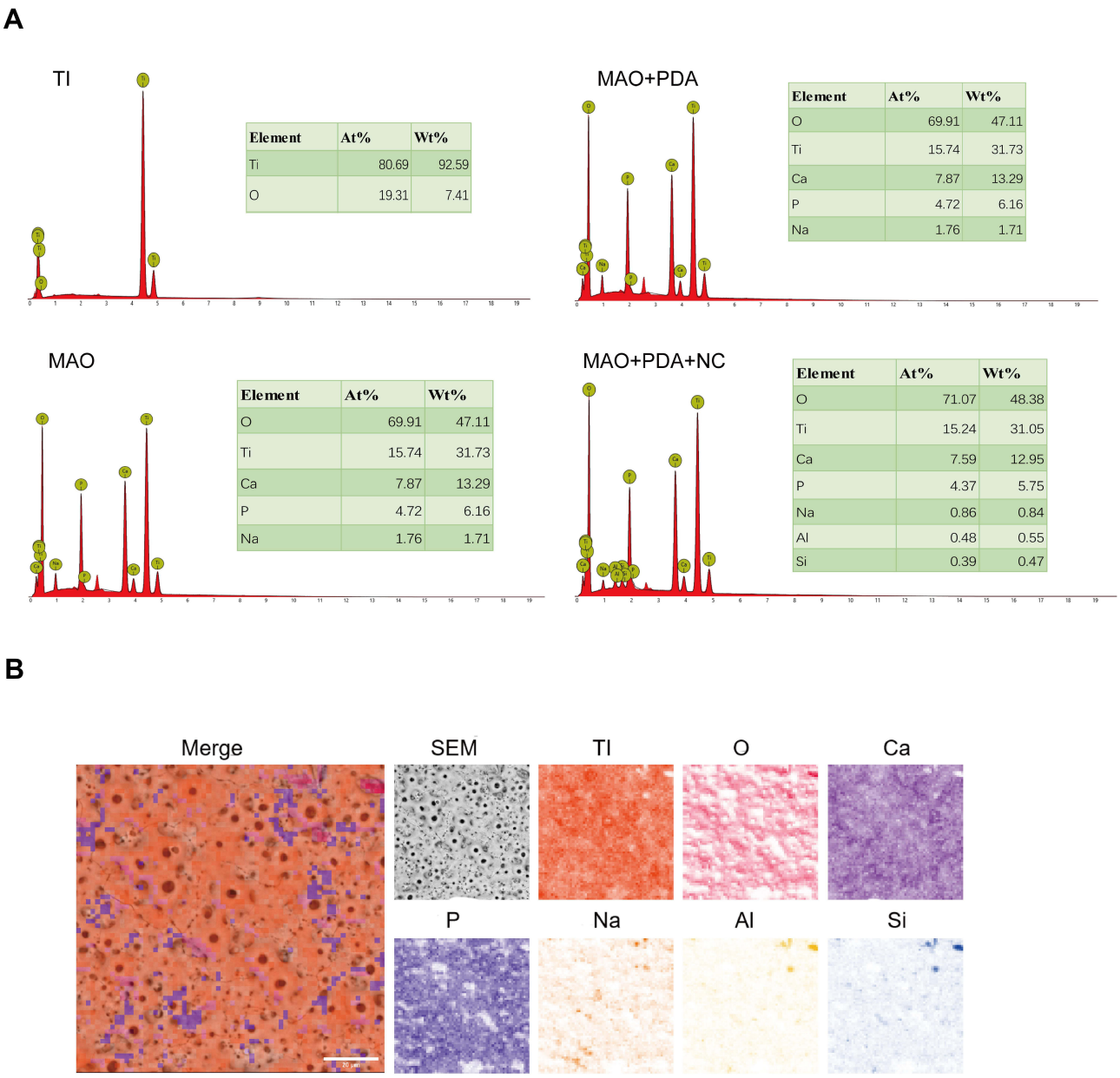

Figure 2 EDS determination of the elemental composition of the coatings.
Notes: (**A**) EDS elemental analysis of TI, MAO, MAO+PDA, and MAO+PDA+NC. (**B**) Energy-dispersive X-ray spectroscopy analysis of MAO+PDA+NC coating and its mapping of the ions.

of the material can be reduced and hydrophilicity can be improved by introducing PDA coating on the surface of MAO coating.

FTIR spectroscopy verified the successful PDA deposition. The MAO+PDA group had two distinct broad absorption bands at about 3410 cm^{-1} and 1590 cm^{-1}, and the MAO+PDA+NC group also had two distinct broad absorption bands at about 3470 cm^{-1} and 1730 cm^{-1} (Figure 3C). All of the FTIR spectra exhibited a broad band at 3470 cm^{-1}, 3410 cm^{-1} that can be assigned to intermolecular hydrogen-bonded O-H stretch with the N-H stretch of secondary amine buried underneath. The band at 1730 cm^{-1} corresponding to C=O stretching vibration and the band at 1590 cm^{-1} that can be attributed to the aromatic ring stretching vibration of the polyindole structures. The samples were immersed in PBS for 1, 3, and 7 days, and the release of ionic elements from the different coatings was examined using ICP-OES (Figure 3D). The cumulative release curve shows that, similar to the EDS results in Figure 2, the release amount of Ca and P elements

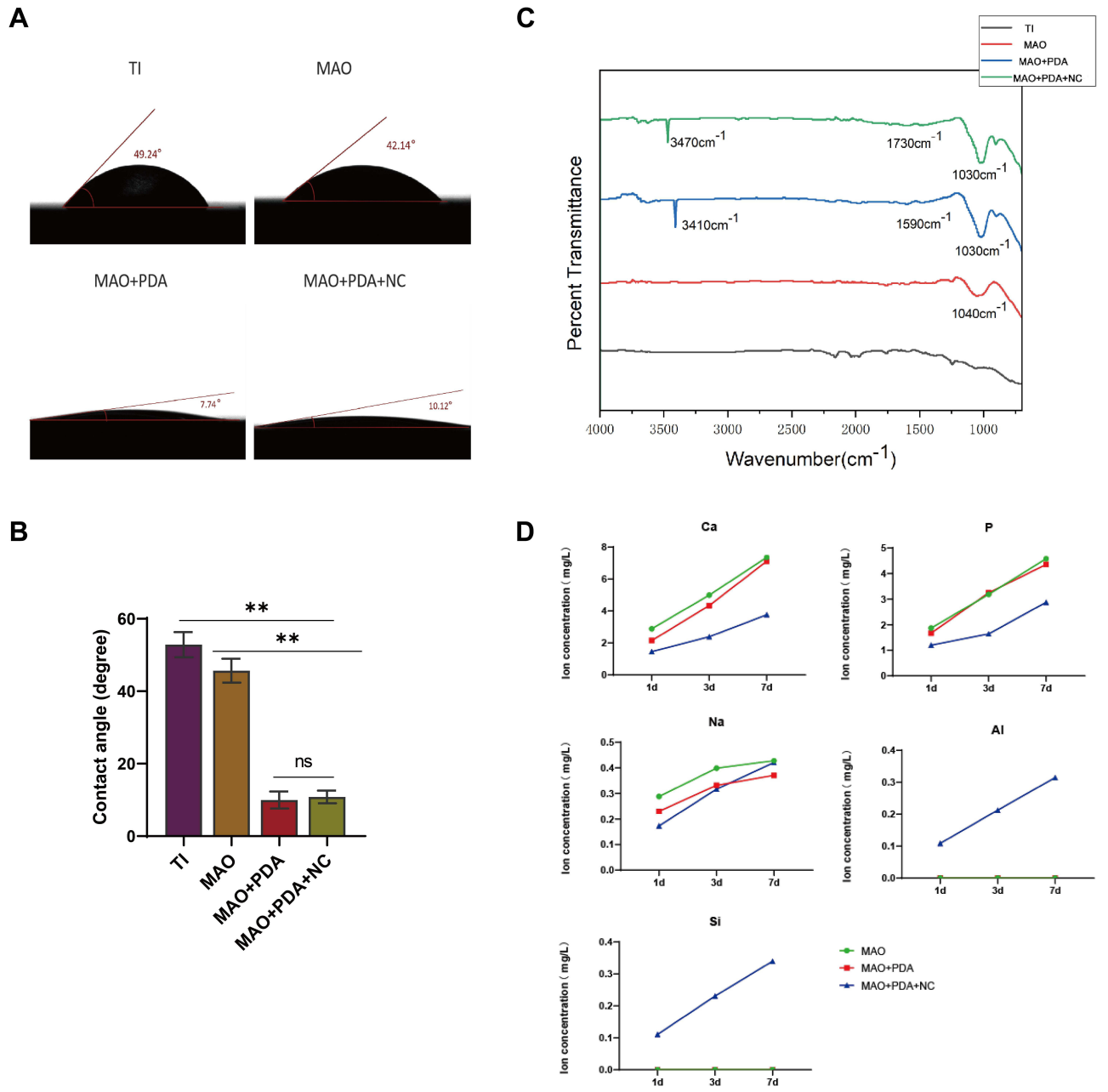

Figure 3 Surface properties of the coatings.

Notes: (**A** and **B**) Surface contact angles of TI, MAO, MAO+PDA, and MAO+PDA+NC. (**C**) ATR–FTIR spectra of samples at the range of 4000–750 cm^{-1}. (**D**) ICP-OES examined the release of different coatings on 1, 3, and 7 days. $^{**}P < 0.01$ indicates significant difference between groups. NS indicates no significant difference between the compared groups.

in the nanoclay is significantly lower than that in the MAO and MAO+PDA groups. In addition, the release of Al, Si and Na elements in the MAO+PDA+NC coating presents a slow and continuous process, in which the release amount of Na element is not significantly different from that of the other two groups, which is attributed to the small amount of Na element in the silicate.

The nanoscratch experiment was performed by probing the surface of the MAO+PDA+NC sample perpendicular to the surface for relative scratching and recording the loading and scratching distance in real time. We find out the most obvious turning point of the curve according to the graph, the Normal Displacement graph shows that the indenter of the scratch at about 50 s-15000 nm does gradually deepen the scratch, and the slope of the curve gradually increases after the 50 s, thus we know that

the coating thickness is about 15000 nm, and the load at this point is called the critical load, the value of 400 mN (Normal Force) (Figure 4A). The coefficient of friction refers to the Lateral Force/Normal Force, which is an index to characterize the friction and wear performance. Generally speaking, the lower the coefficient of friction, the higher the wear resistance under the same conditions. Our experimental results show that the wear resistance of the MAO+PDA+NC coating surface is better as the load

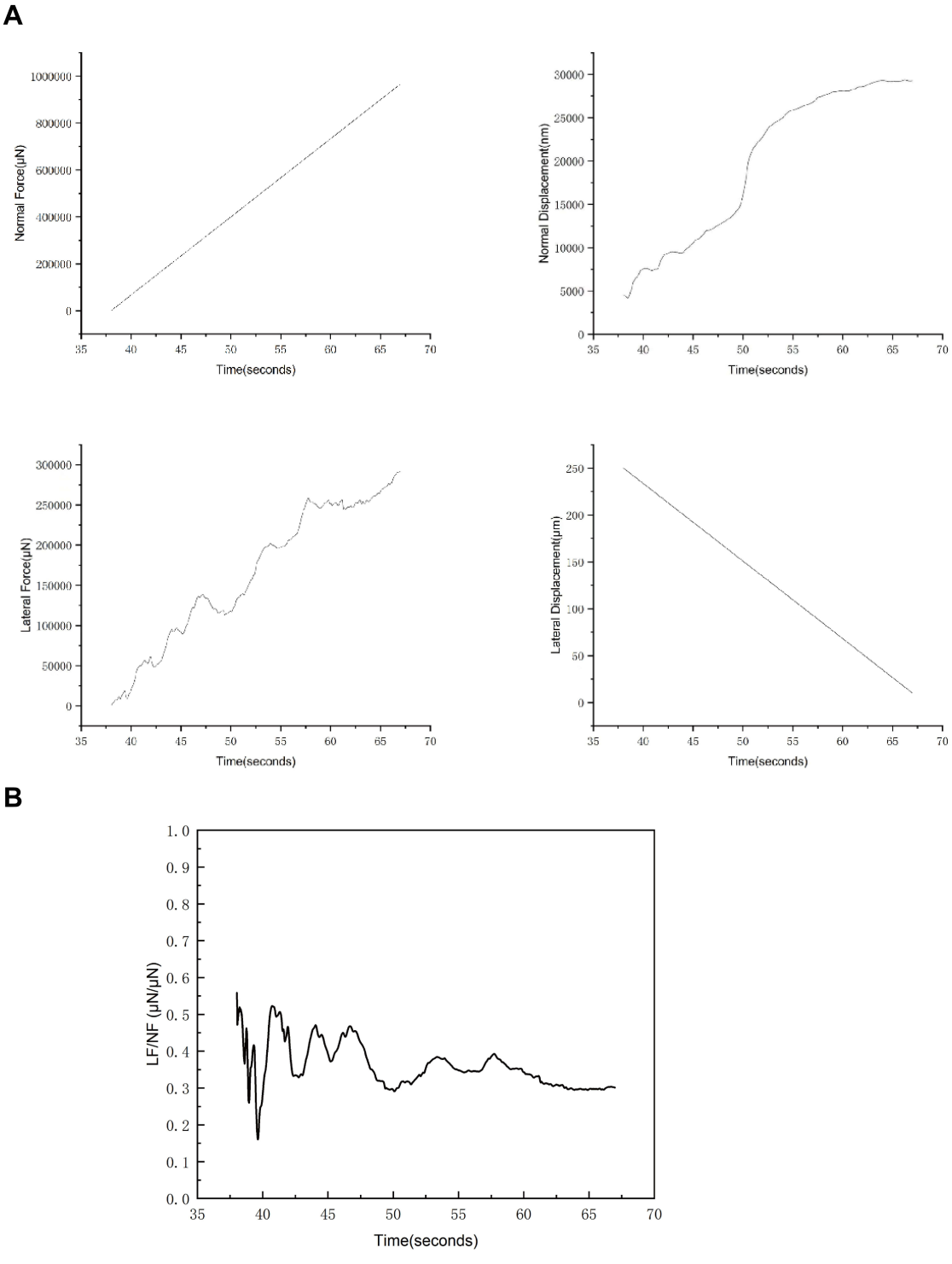

Figure 4 Interfacial bond strength of MAO+PDA+NC coatings.
Notes: (**A**) The thickness of the coating and the critical load are derived from the coordinates corresponding to the curve. (**B**) Friction coefficient refers to the Lateral Force/Normal Force.

increases (Figure 4B). These results indicate that our prepared MAO+PDA+NC coating with a thickness of about 15000 nm has a better interfacial bond strength and better wear resistance.

Cytocompatibility and Biocompatibility of Different Coatings

To assess the potential toxicity of nanoclay nanoparticles, previous studies demonstrated that osteoblasts MC3T3-E1 were placed in different concentrations of Halloysite nanoclay nanoparticles (0.0035–35 mg/mL) and found that Halloysite nanoclay nanoparticles were not toxic to MC3T3-E1 osteoblasts, and thus after administration of the overall cell survival rate remained unchanged after the injection of up to 35 mg/mL Halloysite nanoclay.[17] In this study, the highest concentration of 35 mg/mL nanoclay nanoparticles was taken and soaked on the surface of MAO with the addition of adhesion molecule PDA, and the biocompatibility of MAO+PDA+NC nanocomposite coating was evaluated by using rat bone marrow mesenchymal stem cells. The distribution of the live-dead state of cells on the material after 24 h was observed by staining the surface of different coatings with live and dead cells, where green fluorescence is for live cells and red fluorescence is for dead cells. The results of the live-dead staining images show a large amount of green fluorescence and a small amount of sporadic red fluorescence expression on the surface of the material (Figure 5A), which proves that the modified coatings have no adverse effects on cells and have excellent biocompatibility. The cell proliferation capacity of the nanocomposite coating MAO+PDA+NC was investigated and the results indicated that BMSCs grew on this coating showed a time-dependent growth trend throughout the culture period (1, 3, and 5 days), with the MAO+PDA+NC group showing significantly higher proliferation activity on days 3 and 5 than all other groups (Figure 5B). The cytoskeletal morphology was observed after 1 day of incubation on the surface of different samples, and it was found that good cytoskeletal extension and cell attachment were observed in the MAO+PDA+NC group compared to all other groups (Figure 5C), thus confirming that the MAO+PDA+NC coating facilitated cell attachment and growth. All these results confirm that our nanocomposite coatings can support cell attachment and proliferation with good cytocompatibility as well as biocompatibility for controlling cell function in tissue engineering applications.

Cell Adhesion of Different Coatings

Our next experiments verified the powerful adhesion effect of PDA by detecting the expression of integrin family gene and Vinculin proteins. BMSCs cells were divided into different groups for inoculation, and immunofluorescence staining confirmed the expression of Vinculin protein. After 3 days of culture, the fluorescence intensity of MAO+PDA and MAO +PDA+NC groups was significantly higher than the other groups (Figure 6A). The effects of different coatings on the expression of cell-associated adhesion factors were subsequently examined by RT-PCR. The results showed that the expression of Integrin β3, α2, α3, and α4 in MAO+PDA and MAO+PDA+NC groups were significantly higher than those in TI and MAO groups (Figure 6B). Among them, the MAO+PDA group showed the best adhesion effect, which was weakened after the addition of nanoclay, and it was speculated that this might be caused by the space limitation of nanoclay-induced PDA oxidation.

Effect of Different Coatings on Osteogenic Differentiation

After determining that nanoclay is non-toxic to cells and does not damage cell membranes, we performed extensive osteogenic differentiation experiments to determine the role of nanoclay in the osteogenic differentiation of BMSCs. Our research results showed that the expression of ALP, OPN, Runx2, and OSX osteogenic related genes were significantly upregulated and the expression of Runx2, OCN and OPN protein was increased in the nanoclay modified nanocomposite coating compared to the non-NC treated cells; however, the expression of osteogenic genes and protein was lowest in the TI group (Figure 7A–D). Overall, our results confirmed that the MAO+PDA+NC coating possessed good osteogenic differentiation and that the TI group had the weakest osteogenic effect. To further validate the bioactive characteristics of MAO+PDA+NC coating in promoting and enhancing the osteogenic phenotype of BMSCs, we chose to culture the cells using a standard growth medium without osteoinductive factors (such as dexamethasone) and assayed the ALP activity of this coating. ALP activity is associated with osteoblast differentiation and greatly influences the process of cell matrix mineralization in osteoblasts.[18] In the normal medium, we observed the effects of MAO, MAO+PDA, and MAO+PDA +NC coatings on ALP activity during culture, in which ALP activity was significantly increased in the MAO+PDA+NC

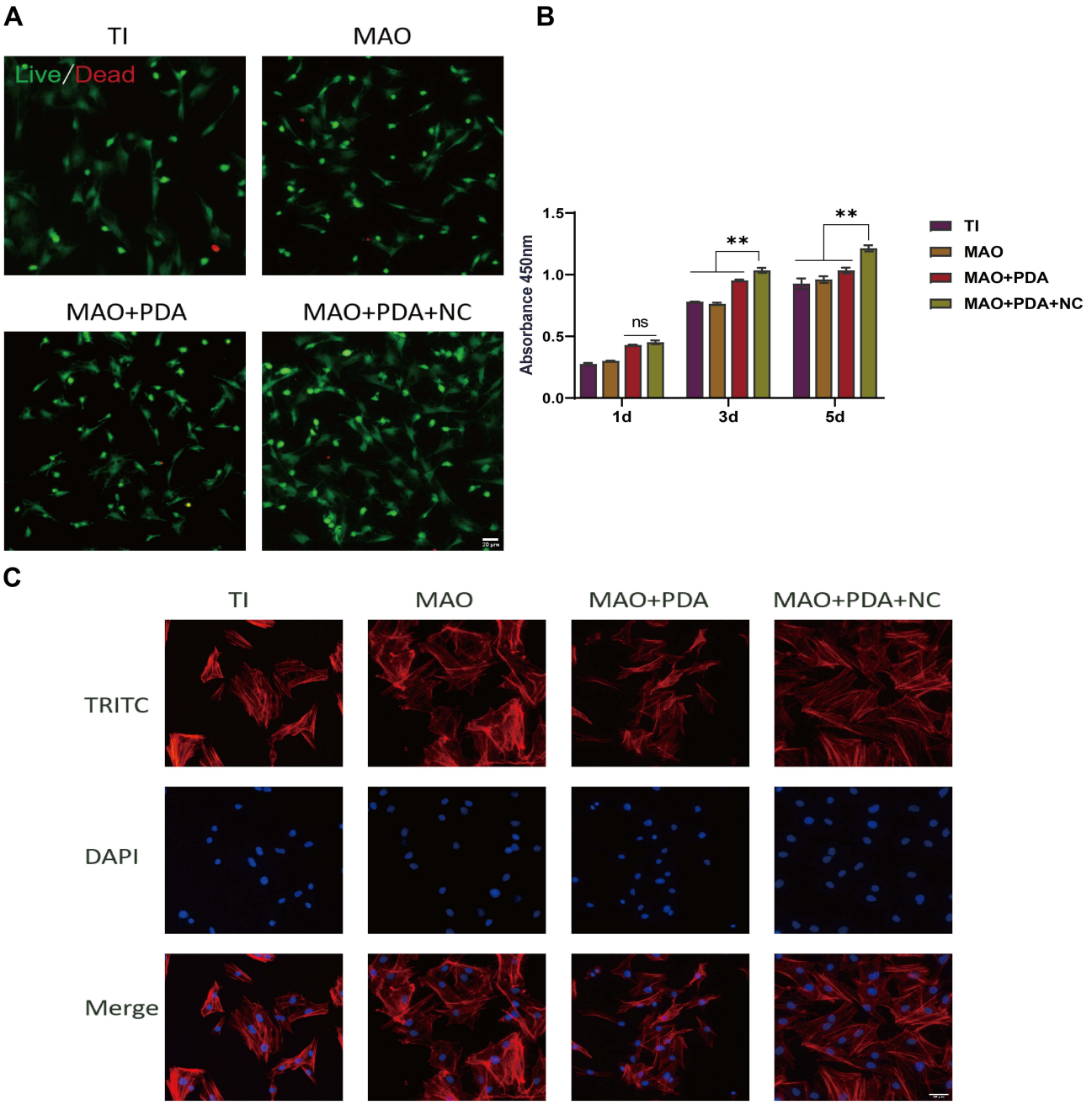

Figure 5 Biocompatibility and cytocompatibility of the different coatings.
Notes: (**A**) Live (green)−Dead (red) cell staining and statistical analysis of BMSCs cultured on the titanium surface of different groups for 1 day. (**B**) BMSCs were cultured in different groups for CCK-8 analysis. (**C**) Fluorescence image analysis of cytoskeletal morphology on various coating surfaces. $^{**}P < 0.01$ indicates a significant difference between MAO+PDA+NC and other groups; NS indicates no significant difference between the compared groups. Scale bar: 100 μm.

group (Figure 7E and F), which further demonstrated that the MAO+PDA+NC composite coating has better osteoinductive activity.

Effect of Ion Release from MAO+PDA+NC Coating Surface on Osteogenesis

Nanoclay has been widely used to enhance bioactivity and osteogenesis on the surface of biomaterials, but the mechanism by which it works has not been determined. Previous studies have shown that bioactive ions released from nanoclay scaffolds/hydrogels form an inducible microenvironment that stimulates osteogenic differentiation of primary

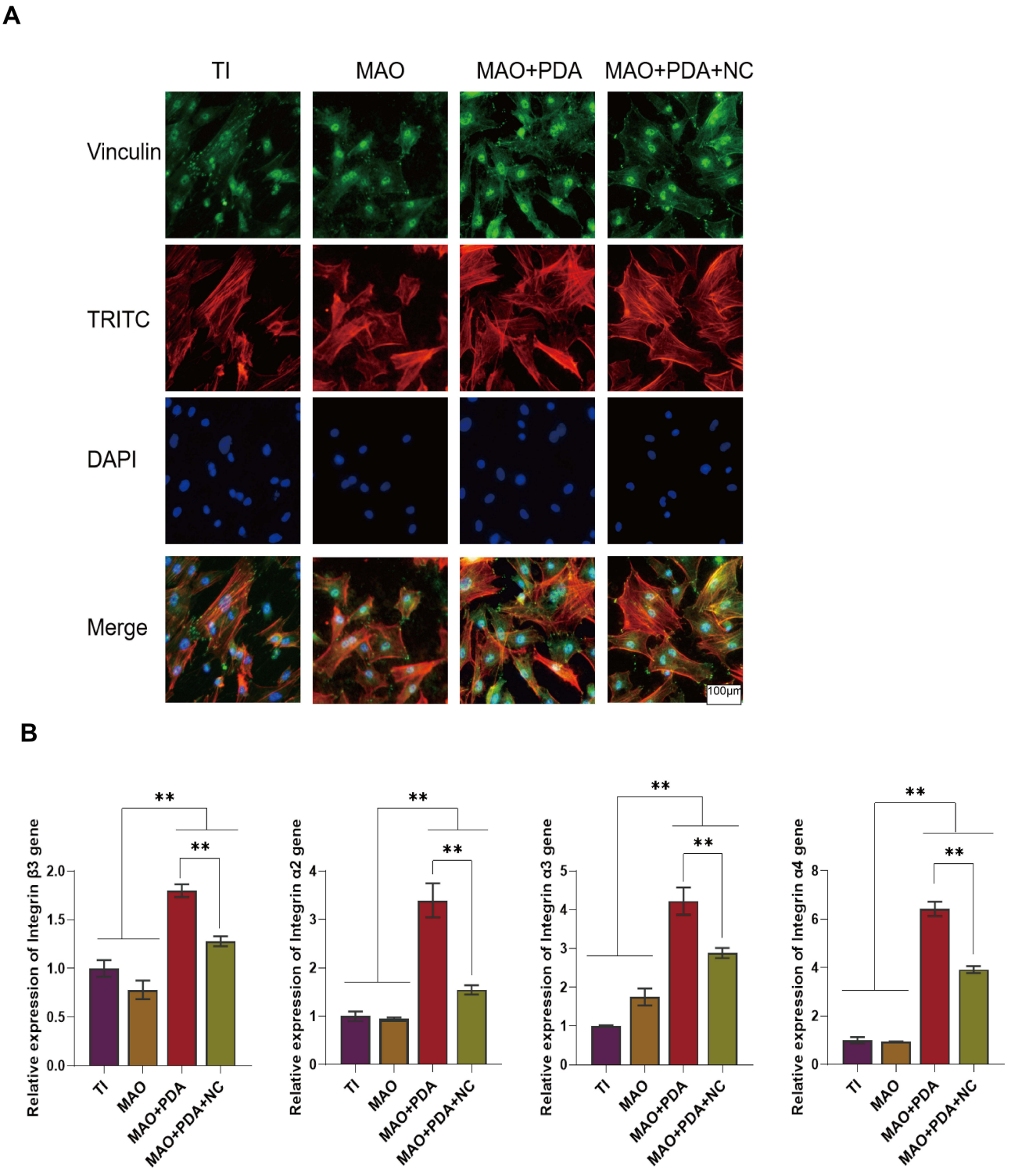

Figure 6 Adhesion of the different coatings.
Notes: (**A**) Vinculin expression detected by an immunofluorescence staining method. (**B**) Expression of the Integrin adhesion-associated genes Integrin β3, Integrin α2, Integrin α3, and Integrin α4. $^{**}P < 0.01$ indicates significant difference between groups. Scale bar: 100μm.

rat osteoblasts (ROBs), thereby promoting bone regeneration.[19,20] Therefore, we further verified the effect of bioactive ions released by nanoclay breakdown on osteogenic differentiation. We chose to place samples from each group into a medium without antibiotics and serum and collected the extracts after 7 days and cultured the cells in the presence of

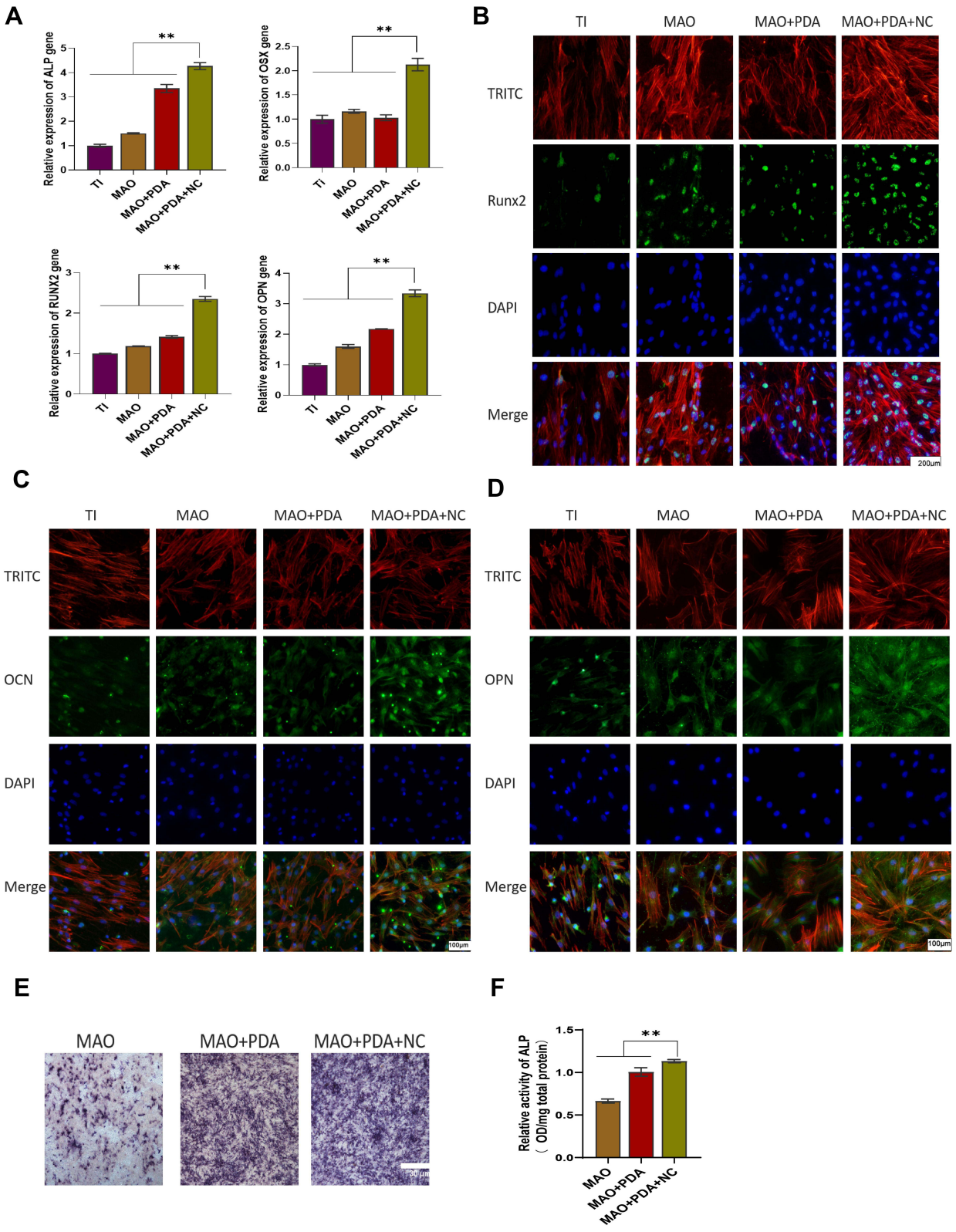

Figure 7 Osteogenic induction of the different coatings.

Notes: (**A**) Expression of the bone-related gene of ALP, OSX, Runx2, and OPN. (**B**–**D**) Runx2, OCN and OPN expression was detected by an immunofluorescence staining method. (**E** and **F**) ALP staining of BMSCs on different templates and quantitative analysis. $^{**}P < 0.01$ indicates significant difference between groups. Scale bar: 30μm and 100μm.

serum and antibiotics. The ALP staining and semi-quantitative results showed that the ALP activity was significantly upregulated in the added nanoclay group compared to all other groups. While there was no significant difference between TI and blank control groups, there was also no significant difference in ALP activity between MAO+PDA and MAO groups due to the similar ionic elements released (Figure 8A and B). In addition, RT-PCR results showed that the expression of osteogenic genes Runx2, OCN, and OPN was upregulated due to the addition of nanoclay compared to other groups (Figure 8C). Fluorescence staining results showed that OPN protein expression was more obvious in MAO +PDA+NC group (Figure 8D). In conclusion, these results suggest that the presence of ionic elements in nanoclay is responsible for enhancing bone healing and stimulating bone formation.

Discussion

To improve the biological and mechanical properties of the surface of titanium implants, many studies have been conducted on the morphological modification of the surface of oral implants. The means of modification of the material surface mainly involves physical modification, chemical modification, and biological modification. Different functionalized nano-coatings are prepared by modifying the surface of titanium implants to create a good microenvironment for promoting bone regeneration.[21–23] Among them, micro-arc oxidation technology is used to mix various chemical elements by adjusting the electrolyte composition, thus preparing an MAO active coating containing micron or nanoscale porous morphology to stimulate osteoblasts to perform normal biological functions and promote osseointegration.[24] However, studies have reported that simple micro- and nanoporous structures cannot fully satisfy the need for osseointegration,[25] and the adhesion properties of the coating surface need to be further confirmed. Therefore, it is particularly essential to prepare a new MAO active coating that can both increase the adhesion of the material surface and meet the requirements of osseointegration for ensuring successful implant placement in the defect area.

Nanoclay is a novel nanomaterial with stable mechanical and biological properties, which not only has excellent osteoinductive properties but also can enhance the interaction with polymers and bioactive components through its unique charge properties.[8–11] For example, charged groups on the polymer backbone can form covalent bonds with the nanoclay surface through electrostatic interactions, where the nanoclay acts as a crosslinking center and individual particles are connected to multiple polymer chains, thus forming a physical crosslinking network.[8,16] In addition, the polymer structure, molecular weight, and hydrophilicity also determine the interaction between nanoclay and polymer.[26,27] Notably, inspired by the powerful wet adhesion properties of mussels, the biopolymer PDA has entered the limelight. Due to its rich content of reactive functional groups, PDA not only has unique adhesion properties but also superior hydrophilic properties.[28–30] It has been shown that nanoclay can induce the oxidation of dopamine to form PDA-clay nanosheets rich in catechol groups, which contributes to the uniform distribution of nanoclay in the polymer network and further enhances mechanical and adhesion properties.[16] Given this, we envisioned a new composite coating by embedding PDA-clay nano layers into MAO active coating, so that this composite coating can achieve both adhesion and osteogenesis effects.

Nanostructural modifications on the surface of the titanium implant material, while leading to an increase in surface roughness, also change the hydrophobic state of the surface, providing more binding sites for the cells.[31,32] From the perspective of surface microscopic roughness, by introducing a nanoclay component to the MAO coating surface, the roughness of the material surface increases, which can better simulate a cellular environment suitable for rapid alveolar bone growth. From the perspective of material surface wettability, poor material surface wettability, poor cell affinity, and poor cell adhesion, and the introduction of hydrophilic substances to reduce surface tension is an effective means to improve cell affinity.[33] In addition, the active coating on the implant surface provides the conditions needed for osteoblasts to proliferate and promote new bone formation.[34,35] The results of our cell proliferation experiments showed that MAO+PDA+NC nanocomposite coating had no adverse effects on cells and was able to promote cell proliferation and growth, and skeleton staining revealed that cells spread completely on the surface of the coating, proving good surface interface compatibility between the coating and cells, which is conducive to cell attachment and adhesion.

The nanosized surface of the titanium implant material has a greater influence on the adhesion of the cells. When cells adhere to the material surface, they are firstly adsorbed on the material surface by cell adhesion proteins, which bind to cell membrane receptors before mediating cell adhesion, and such adhesion is more conducive to osteoblast differentiation and bone tissue regeneration.[36–38] Vinculin is an actin-binding protein that forms an adhesion complex based on calmodulin and

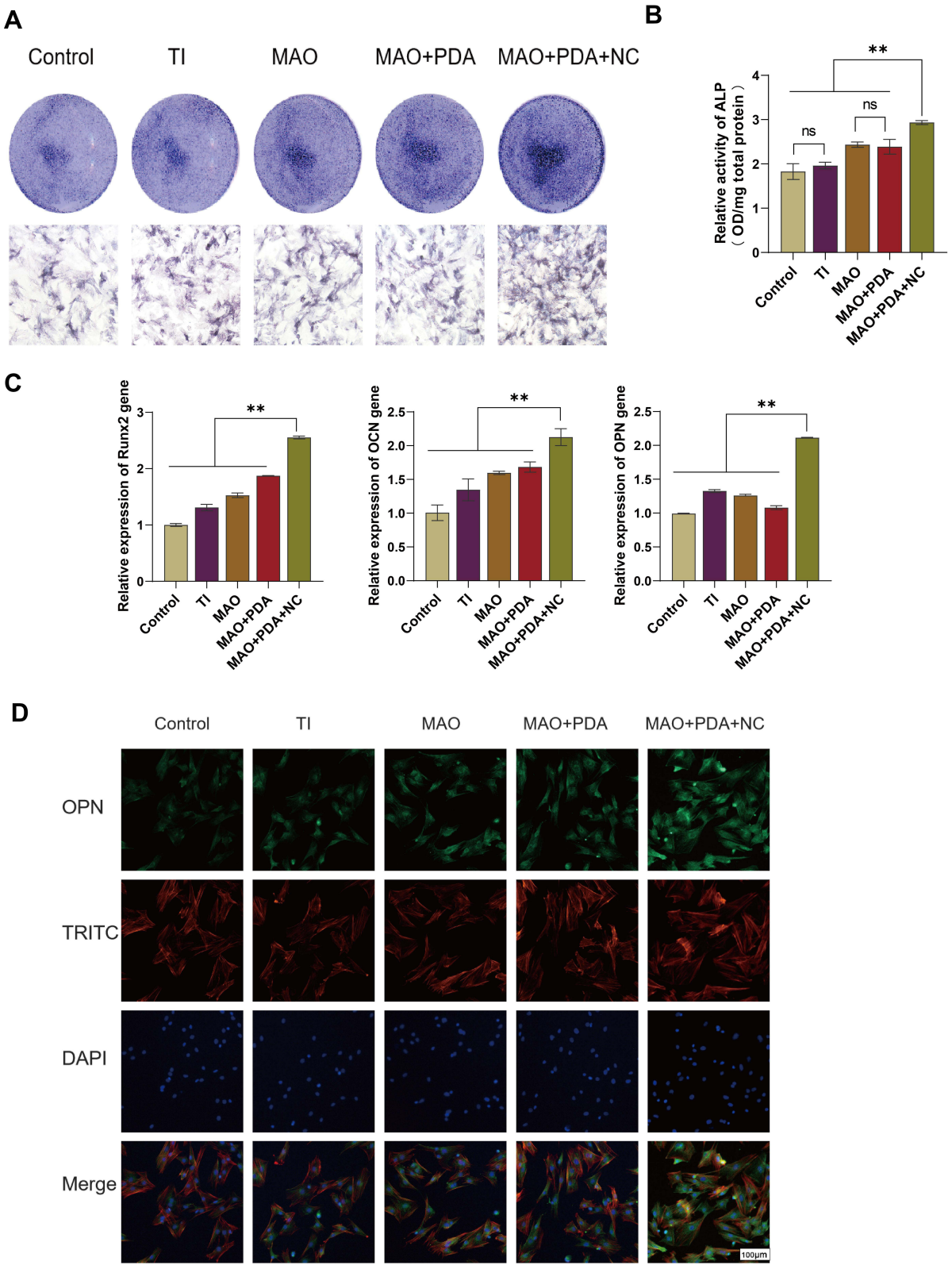

Figure 8 Osteogenic induction of active ions released from the different coatings.
Notes: (**A** and **B**) ALP staining of BMSCs on different groups and quantitative analysis. (**C**) Expression of the bone-related gene of Runx2, OCN, and OPN. (**D**) OPN expression was detected by an immunofluorescence staining method. $^{**}P < 0.01$ indicates significant difference between groups.

integrins and is thought to enhance intercellular and extracellular matrix adhesion.[39] Integrins are transmembrane heterodimers composed of α and β subunits, a family of adhesion molecules that sense, respond to, and interact with different extracellular matrix components with high specificity, mediating adhesion between cells and the extracellular matrix.[40] Our study verified the adhesion of MAO+PDA+NC coated surface by detecting the expression of Vinculin protein and integrin family genes. In addition, it was shown that enhanced cell adhesion and proliferation were associated with improved surface hydrophilicity and the presence of functional groups.[41,42] We also found that due to the richness of PDA coatings in various reactive functional groups and their superior hydrophilicity, the adhesion effect is particularly pronounced when PDA substances are introduced to the surface of MAO coatings. In contrast, with the addition of nanoclay particles with high specific surface area, the interfacial bonding between the clay and PDA coating leads to the formation of physical crosslinks within the nanocomposite network, reducing the number of chemical crosslinks required for network formation, while at the same time, the oxidation of PDA in the nanoclay layer is limited, making the free catechol groups interacting with nanoclay require a higher fracture to separate the bonded joints and their adhesion would be compromised.[43,44] In conclusion, the introduction of different material compositions and functional groups on the surface of MAO coatings can modulate the adsorption capacity of the cells on the coating surface.

Rapid osseointegration is a key factor in determining the success of dental implants, and porous titanium oxide coatings prepared by MAO have been shown to be an effective method for enhancing osteogenesis; therefore, nanoclay materials with osteoinductive activity were added to evaluate the ability of nanoactive coatings to promote early and rapid interfacial osseointegration of titanium implants. Runx2, OSX, OPN, OCN, and ALP are important osteogenic markers that regulate the formation and differentiation of bone tissue. Among them, Runx2 belongs to the Runx family of transcription factors and is expressed in late mesenchymal condensed and osteochondral progenitor cells of skeletal development and acts as a master regulator of osteogenesis.[45] Osterix (OSX) is thought to be a downstream target of Runx2, acting at later stages of osteogenesis and maturation, controlling the maturation of functional osteoblasts and further differentiation towards osteocytes.[45,46] OPN and OCN are involved in the late stages of osteogenic differentiation. And OPN is an extracellular structural protein that is secreted and synthesized by preosteoblasts, osteoblasts and osteocytes and is thought to be important for bone remodeling.[10] ALP is an early indicator of the osteogenic phenotype and plays an important role in the initial stages of bone matrix mineralization.[47] Our study compared the osteogenic differentiation of various coatings. At the protein level, immunofluorescence staining showed that the expression of both Runx2, OCN and OPN in the MAO+PDA+NC group was significantly better than that in the control group; at the gene level, RT-PCR detected significantly higher expression of Runx2, ALP, OSX, and OPN genes in the MAO+PDA+NC group than in the other groups; at the matrix mineralization level, ALP staining and semi-quantitative results indicated that MAO+PDA+NC coating could significantly promote the mineralization process of osteoblasts and promote bone formation. In addition, previous studies have reported the important role of silicate on osteogenic differentiation. Therefore, we explored the ability of the ionic components of the coating retardation on osteogenic differentiation and mineralization of BMSCs in vitro, and based on the experimental results, we found that the ionic components released from the MAO+PDA+NC group played a more important role in the induction of osteogenic differentiation. We speculate that this may be attributed to the synergistic effect of the silicate ionic component with the elemental component in the micro arc oxidation electrolyte, which needs further verification. These findings suggest that MAO-PDA-NC nanocomposite coatings can enhance osteogenic differentiation of BMSCs toward early and late stages of osteogenesis and promote early and rapid osseointegration of titanium implants.

Conclusions

In this study, we successfully prepared a bioactive nanocomposite coating (MAO-PDA-NC) by micro-arc oxidation technique and confirmed that the coating not only optimizes the physical and chemical properties of the ware surface but also significantly stimulates a variety of biological properties such as adhesion, proliferation and osteogenic differentiation of osteoblasts on the material surface. The new nanocomposite coating provides new insights into the exploration of implant surface nano-modification and is expected to play an active role in the early osseointegration of implant placement. Based on this study, further exploration of the molecular regulatory mechanisms involved in osseointegration by the MAO-PDA-NC composite coating and the factors that may induce immune responses during this process is needed, which will provide new ideas for future therapeutic targets to improve implant osseointegration.

Ethics Approval and Informed Consent

The study was approved by the Institutional Animal Care and Use Committee of Ninth People's Hospital Affiliated to Shanghai Jiao Tong University (reference no. SH9H-2020-A94-1). All animals were followed by the guidelines of the National Institutes of Health guide for the care and use of laboratory animals (NIH Publications No. 8023, revised 1978).

Acknowledgments

This study was supported by the National Natural Science Foundation of China (No. 32000973) and the Natural Science Foundation of Shandong Province (No.ZR2021MH397).

Disclosure

The authors report no conflicts of interest in this work.

References

1. Chouirfa H, Bouloussa H, Migonney V, et al. Review of titanium surface modification techniques and coatings for antibacterial applications. *Acta Biomater*. 2019;83:37–54. doi:10.1016/j.actbio.2018.10.036
2. Zhao Q, Yi L, Jiang L, Ma Y, Lin H, Dong J. Surface functionalization of titanium with zinc/strontium-doped titanium dioxide microporous coating via microarc oxidation. *Nanomedicine*. 2019;16:149–161. doi:10.1016/j.nano.2018.12.006
3. Bharadwaz A, Jayasuriya AC. Recent trends in the application of widely used natural and synthetic polymer nanocomposites in bone tissue regeneration. *Mater Sci Eng C Mater Biol Appl*. 2020;110:110698. doi:10.1016/j.msec.2020.110698
4. Wang X, Mei L, Jiang X, et al. Hydroxyapatite-coated titanium by micro-arc oxidation and steam-hydrothermal treatment promotes osseointegration. *Front Bioeng Biotechnol*. 2021;9:625877. doi:10.3389/fbioe.2021.625877
5. Hameed P, Gopal V, Bjorklund S, et al. Axial suspension plasma spraying: an ultimate technique to tailor Ti6Al4V surface with HAp for orthopaedic applications. *Colloids Surf B Biointerfaces*. 2019;173:806–815. doi:10.1016/j.colsurfb.2018.10.071
6. Lopes JH, Bueno OM, Mazali IO, et al. Investigation of citric acid-assisted sol-gel synthesis coupled to the self-propagating combustion method for preparing bioactive glass with high structural homogeneity. *Mater Sci Eng C Mater Biol Appl*. 2019;97:669–678. doi:10.1016/j.msec.2018.12.022
7. Yin S, Sun N, Jiang F, et al. The translation from in vitro bioactive ion concentration screening to in vivo application for preventing peri-implantitis. *ACS Appl Mater Interfaces*. 2021;13(4):5782–5794. doi:10.1021/acsami.0c19698
8. Gaharwar AK, Cross LM, Peak CW, et al. 2D nanoclay for biomedical applications: regenerative medicine, therapeutic delivery, and additive manufacturing. *Adv Mater*. 2019;31(23):e1900332. doi:10.1002/adma.201900332
9. Lee CS, Hwang HS, Kim S, et al. Inspired by nature: facile design of nanoclay-organic hydrogel bone sealant with multifunctional properties for robust bone regeneration. *Adv Funct Mater*. 2020;30(43):2003717. doi:10.1002/adfm.202003717
10. Gaharwar AK, Mihaila SM, Swami A, et al. Bioactive silicate nanoplatelets for osteogenic differentiation of human mesenchymal stem cells. *Adv Mater*. 2013;25(24):3329–3336. doi:10.1002/adma.201300584
11. Xavier JR, Thakur T, Desai P, et al. Bioactive nanoengineered hydrogels for bone tissue engineering: a growth-factor-free approach. *ACS Nano*. 2015;9(3):3109–3118. doi:10.1021/nn507488s
12. Xie M, Zheng Z, Pu S, et al. Macroporous adhesive nano-enabled hydrogels generated from air-in-water emulsions. *Macromol Biosci*. 2022;22(4):e2100491. doi:10.1002/mabi.202100491
13. Shi M, Zhang J, Li J, et al. Polydopamine-coated magnetic mesoporous silica nanoparticles for multimodal cancer theranostics. *J Mater Chem B*. 2019;7(3):368–372. doi:10.1039/C8TB03021A
14. Xie X, Tang J, Xing Y, et al. Intervention of polydopamine assembly and adhesion on nanoscale interfaces: state-of-the-art designs and biomedical applications. *Adv Healthc Mater*. 2021;10(9):e2002138. doi:10.1002/adhm.202002138
15. Batul R, Tamanna T, Khaliq A, et al. Recent progress in the biomedical applications of polydopamine nanostructures. *Biomater Sci*. 2017;5(7):1204–1229. doi:10.1039/C7BM00187H
16. Han L, Lu X, Liu K, et al. Mussel-inspired adhesive and tough hydrogel based on nanoclay confined dopamine polymerization. *ACS Nano*. 2017;11(3):2561–2574. doi:10.1021/acsnano.6b05318
17. Gaharwar AK, Schexnailder PJ, Kline BP, et al. Assessment of using laponite cross-linked poly(ethylene oxide) for controlled cell adhesion and mineralization. *Acta Biomater*. 2011;7(2):568–577. doi:10.1016/j.actbio.2010.09.015
18. Liao F, Hu X, Chen R. The effects of Omarigliptin on promoting osteoblastic differentiation. *Bioengineered*. 2021;12(2):11837–11846. doi:10.1080/21655979.2021.1999366
19. Zhai X, Ruan C, Ma Y, et al. 3D-bioprinted osteoblast-laden nanocomposite hydrogel constructs with induced microenvironments promote cell viability, differentiation, and osteogenesis both in vitro and in vivo. *Adv Sci*. 2017;5(3):1700550. doi:10.1002/advs.201700550
20. Zhai X, Ruan C, Shen J, et al. Clay-based nanocomposite hydrogel with attractive mechanical properties and sustained bioactive ion release for bone defect repair. *J Mater Chem B*. 2021;9(10):2394–2406. doi:10.1039/D1TB00184A
21. Wang J, Zhi D, Zhou H, et al. Evaluating tetracycline degradation pathway and intermediate toxicity during the electrochemical oxidation over a Ti/Ti_4O_7 anode. *Water Res*. 2018;137:324–334. doi:10.1016/j.watres.2018.03.030
22. Wang Z, Mei L, Liu X, et al. Hierarchically hybrid biocoatings on Ti implants for enhanced antibacterial activity and osteogenesis. *Colloids Surf B Biointerfaces*. 2021;204:111802. doi:10.1016/j.colsurfb.2021.111802
23. Shi A, Cai D, Hu J, et al. Development of a low elastic modulus and antibacterial Ti-13Nb-13Zr-5Cu titanium alloy by microstructure controlling. *Mater Sci Eng C Mater Biol Appl*. 2021;126:112116. doi:10.1016/j.msec.2021.112116
24. He W, Yin X, Xie L, et al. Enhancing osseointegration of titanium implants through large-grit sandblasting combined with micro-arc oxidation surface modification. *J Mater Sci Mater Med*. 2019;30(6):73. doi:10.1007/s10856-019-6276-0

25. Li X, Wang M, Zhang W, et al. A magnesium-incorporated nanoporous titanium coating for rapid osseointegration. *Int J Nanomedicine*. 2020;15:6593–6603. doi:10.2147/IJN.S255486
26. Gaharwar AK, Schexnailder PJ, Dundigalla A, et al. Highly extensible bio-nanocomposite fibers. *Macromol Rapid Commun*. 2011;32(1):50–57. doi:10.1002/marc.201000556
27. Lu P, Wang G, Qian T, et al. The balanced microenvironment regulated by the degradants of appropriate PLGA scaffolds and chitosan conduit promotes peripheral nerve regeneration. *Mater Today Bio*. 2021;12:100158. doi:10.1016/j.mtbio.2021.100158
28. Pandey N, Soto-Garcia L, Yaman S, et al. Polydopamine nanoparticles and hyaluronic acid hydrogels for mussel-inspired tissue adhesive nanocomposites. *Mater Sci Eng C Mater Biol Appl*. 2021;134:112589.
29. Xie L, Cui X, Liu J, et al. Nanomechanical insights into versatile polydopamine wet adhesive interacting with liquid-infused and solid slippery surfaces. *ACS Appl Mater Interfaces*. 2021;13(5):6941–6950. doi:10.1021/acsami.0c22073
30. Feng P, Peng S, Shuai C, et al. In situ generation of hydroxyapatite on biopolymer particles for fabrication of bone scaffolds owning bioactivity. *ACS Appl Mater Interfaces*. 2020;12(41):46743–46755. doi:10.1021/acsami.0c13768
31. Jemat A, Ghazali MJ, Razali M, et al. Surface modifications and their effects on titanium dental implants. *Biomed Res Int*. 2015;2015:791725. doi:10.1155/2015/791725
32. Lorenzetti M, Dogša I, Stošicki T, et al. The influence of surface modification on bacterial adhesion to titanium-based substrates. *ACS Appl Mater Interfaces*. 2015;7(3):1644–1651. doi:10.1021/am507148n
33. Gittens RA, Olivares-Navarrete R, Cheng A, et al. The roles of titanium surface micro/nanotopography and wettability on the differential response of human osteoblast lineage cells. *Acta Biomater*. 2013;9(4):6268–6277. doi:10.1016/j.actbio.2012.12.002
34. Costa DG, Ferraz EP, Abuna RPF, et al. The effect of collagen coating on titanium with nanotopography on in vitro osteogenesis. *J Biomed Mater Res A*. 2017;105(10):2783–2788. doi:10.1002/jbm.a.36140
35. Lin DJ, Fuh LJ, Chen CY, et al. Rapid nano-scale surface modification on micro-arc oxidation coated titanium by microwave-assisted hydrothermal process. *Mater Sci Eng C Mater Biol Appl*. 2019;95:236–247. doi:10.1016/j.msec.2018.10.085
36. Jones MC, Zha J, Humphries MJ. Connections between the cell cycle, cell adhesion and the cytoskeleton. *Philos Trans R Soc Lond B Biol Sci*. 2019;374(1779):20180227. doi:10.1098/rstb.2018.0227
37. Chen S, Guo Y, Liu R, et al. Tuning surface properties of bone biomaterials to manipulate osteoblastic cell adhesion and the signaling pathways for the enhancement of early osseointegration. *Colloids Surf B Biointerfaces*. 2018;164:58–69. doi:10.1016/j.colsurfb.2018.01.022
38. Chen Q, Zhang D, Zhang W, et al. Dual mechanism β-amino acid polymers promoting cell adhesion. *Nat Commun*. 2021;12(1):562. doi:10.1038/s41467-020-20858-x
39. Huang DL, Bax NA, Buckley CD, et al. Vinculin forms a directionally asymmetric catch bond with F-actin. *Science*. 2017;357(6352):703–706. doi:10.1126/science.aan2556
40. Sun Z, Costell M, Fässler R. Integrin activation by talin, kindlin and mechanical forces. *Nat Cell Biol*. 2019;21(1):25–31. doi:10.1038/s41556-018-0234-9
41. Luna SM, Silva SS, Gomes ME, et al. Cell adhesion and proliferation onto chitosan-based membranes treated by plasma surface modification. *J Biomater Appl*. 2011;26(1):101–116. doi:10.1177/0885328210362924
42. Benhabbour SR, Sheardown H, Adronov A. Cell adhesion and proliferation on hydrophilic dendritically modified surfaces. *Biomaterials*. 2008;29(31):4177–4186. doi:10.1016/j.biomaterials.2008.07.016
43. Liu Y, Meng H, Konst S, Sarmiento R, Rajachar R, Lee BP. Injectable dopamine-modified poly(ethylene glycol) nanocomposite hydrogel with enhanced adhesive property and bioactivity. *ACS Appl Mater Interfaces*. 2014;6(19):16982–16992. doi:10.1021/am504566v
44. Yu L, He T, Yao J, et al. Cu ions and cetyltrimethylammonium bromide loaded into montmorillonite: a synergistic antibacterial system for bone scaffolds. *Mater Chem Front*. 2022;6:103–116. doi:10.1039/D1QM01278A
45. Chan WCW, Tan Z, To MKT, et al. Regulation and role of transcription factors in osteogenesis. *Int J Mol Sci*. 2021;22(11):5445. doi:10.3390/ijms22115445
46. Shi L, Cai G, Shi J, et al. Ossification of the posterior ligament is mediated by osterix via inhibition of the β-catenin signaling pathway. *Exp Cell Res*. 2016;349(1):53–59. doi:10.1016/j.yexcr.2016.09.019
47. Guo Z, Dong L, Xia J, et al. 3D printing unique nanoclay-incorporated double-network hydrogels for construction of complex tissue engineering scaffolds. *Adv Healthc Mater*. 2021;10(11):e2100036. doi:10.1002/adhm.202100036